Manipulating Biphotonic Qutrits

B. P. Lanyon,[1] T. J. Weinhold,[1] N. K. Langford,[1] J. L. O'Brien,[2] K. J. Resch,[3] A. Gilchrist,[1] and A. G. White[1]

[1]*Department of Physics and Centre for Quantum Computer Technology, University of Queensland, Brisbane, Australia*

[2]*Centre for Quantum Photonics, H. H. Wills Physics Laboratory and Department of Electrical and Electronic Engineering, University of Bristol, Bristol, United Kingdom*

[3]*Institute for Quantum Computing and Department of Physics & Astronomy, University of Waterloo, Waterloo, Canada*

(Received 18 July 2007; published 14 February 2008)

Quantum information carriers with higher dimension than the canonical qubit offer significant advantages. However, manipulating such systems is extremely difficult. We show how measurement-induced nonlinearities can dramatically extend the range of possible transforms on biphotonic qutrits—three-level quantum systems formed by the polarization of two photons in the same spatiotemporal mode. We fully characterize the biphoton-photon entanglement that underpins our technique, thereby realizing the first instance of qubit-qutrit entanglement. We discuss an extension of our technique to generate qutrit-qutrit entanglement and to manipulate any bosonic encoding of quantum information.

DOI: 10.1103/PhysRevLett.100.060504 PACS numbers: 03.67.Mn, 03.65.Ud, 03.65.Wj, 42.50.Dv

Higher dimensional systems offer advantages such as increased security in a range of quantum information protocols [1–7], greater channel capacity for quantum communication [8], novel fundamental tests of quantum mechanics [9,10], and more efficient quantum gates [11]. Optically such systems have been realized using polarization [12] and transverse spatial modes [1,13]. However in each case state transformation techniques have proved difficult to realize. In fact, performing such transformations is a significant problem in a range of physical architectures.

The polarization of two photons in the same spatiotemporal mode represents a three-level bosonic quantum system, a biphotonic qutrit, with symmetric logical basis states: $|0_3\rangle \equiv |2_H, 0_V\rangle$, $|1_3\rangle \equiv (|1_H, 1_V\rangle + |1_V, 1_H\rangle)/\sqrt{2}$, and $|2_3\rangle \equiv |0_H, 2_V\rangle$ [14]. The simple optical tools which allow full control over the polarization of a photonic qubit are insufficient for full control over a biphotonic qutrit [15]. Consequently even simple state transformations required in qutrit generation, processing, and measurement are extremely limited. Significant progress has been made in biphoton state generation. For example, complex arbitrary state preparation techniques that employ multiple nonlinear crystals [12] and nonmaximally entangled states [16] have been developed.

Here we present and demonstrate a technique that dramatically extends the range of biphotonic qutrit transforms, for use in all stages of qutrit manipulation. The technique is based on a Fock-state filter which employs a measurement-induced nonlinearity to conditionally remove photon number (Fock) states from superpositions [17–22]. We first demonstrate the action of the filter as a qutrit polarizer, which can conditionally remove a single logical qutrit state from a superposition. We then combine this nonlinear operation with standard wave plate rotations to demonstrate the dramatically increased range of qutrit transforms it enables. Finally we present the first instance and full characterization of a polarization entangled photon-biphoton state, which underpins the power of our technique. Such qubit-qutrit states have been studied extensively [23–29] and we suggest an extension to generate this type of entanglement.

We generate our qutrits through double-pair emission from spontaneous parametric down-conversion (Fig. 1). Fourfold coincidences between detectors D1–D4 select, with high probability, the cases of double-pair emission into inputs 1 and 2. The biphoton state in mode 1 is passed through a horizontal polarizer to prepare the logical qutrit state $|0_3\rangle$. Input 2 is passed through a 50% beam splitter; detection at D1 indicates a single photon in mode b; after a polarizing beam splitter this prepares the ancilla polarization qubit ($|0_2\rangle \equiv |1_H\rangle$, $|1_2\rangle \equiv |1_V\rangle$) in the logical state $|0_2\rangle$. Thus a qubit and qutrit arrive simultaneously at the central 50% beam splitter.

A Fock filter relies on nonclassical interference effects [30]. When two indistinguishable photons are injected into modes a and b (Fig. 1), the probability of detecting a single photon in mode d is zero; if two or more photons are injected into mode a, then this probability is nonzero. By injecting a single photon into mode b and detecting a single photon in mode d, single photon terms can therefore be removed from any photon number superposition states

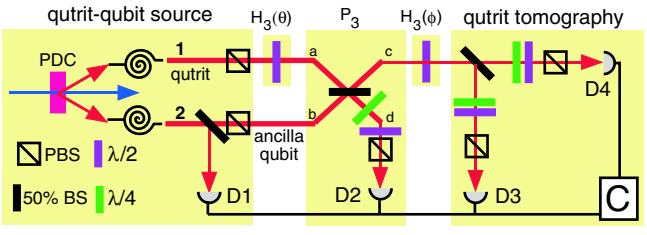

FIG. 1 (color online). Experimental schematic. Emission from a parametric down-conversion (PDC) crystal is coupled into single-mode fiber and injected into modes 1 and 2. Coincident (C) detection of photons at D1–4 selects, with high probability, the cases of double photon-pair emission from the PDC source.

arriving in mode a. By varying the reflectivity of the beam splitter it is possible to conditionally remove any number state from a superposition [21]. This Fock-state filter acts only on light with the same polarization as the ancilla (in our case, horizontal), so by detecting a single horizontal photon in mode d, the logical qutrit state $|1_3\rangle$ is blocked, since it contains a single photon with the same polarization as the ancilla. The remaining logical qutrit states are coherently attenuated.

For a beam splitter of reflectivity 50% the filter acts as a qutrit polarizer described by the operator $\mathbf{P}_3 = |0_3\rangle\langle 0_3| - |2_3\rangle\langle 2_3|$. By varying the polarization of the ancilla, and the reflectivity of the central beam splitter, the operation of our lossy qutrit polarizer can be tuned to preferentially remove the $|0_3\rangle$, $|1_3\rangle$, or $|2_3\rangle$ states. We choose to demonstrate removal of the $|1_3\rangle$ state and include the general operation of the filter for an arbitrary beam splitter reflectivity [31].

The qutrit polarizer offers a powerful tool for transforming between qutrit states. For example, consider the initial qutrit state $|0_3\rangle$ injected into input 1, the red dot of Fig. 2. The black ring shows the limited range of qutrit states, with real coefficients, that are accessible using wave plates [32]. By including the qutrit polarizer the range is dramatically extended to the closed sphere in Fig. 2; the transformation to any real state is possible.

We measure our qutrits by passing mode c through a 50% beam splitter and performing polarization analysis of the two outputs in coincidence, as shown in Fig. 1. This nondeterministically discriminates the logical states $|0_3\rangle$, $|1_3\rangle$, and $|2_3\rangle$ with probabilities $p(0_3) = \frac{1}{2}$, $p(1_3) = \frac{1}{4}$, and $p(2_3) = \frac{1}{2}$. Combining it with single qubit rotations after the beam splitter allows us to perform full qutrit state tomography of mode c. Complete qutrit tomography requires nine independent measurements, which we construct from logical basis states and two-part superpositions [1]. Our method differs from that of Refs. [14,15]. We use convex optimization to reconstruct the qutrit density matrix and Monte Carlo simulations for error analysis [33,34].

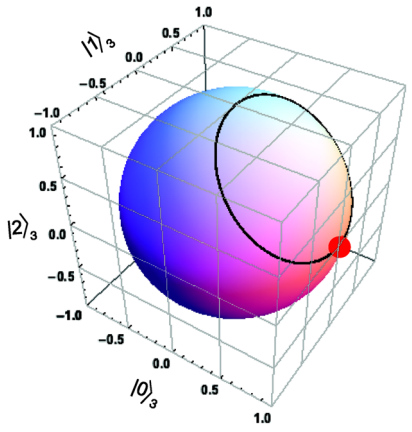

FIG. 2 (color online). Comparison of the range of linearly polarized qutrit states achievable by transforming the state $|0_3\rangle$ (red dot); when using only wave plate operations (black ring); by incorporating our qutrit polarizer, $\mathbf{Q}_3(\alpha)\mathbf{H}_3(\phi)\mathbf{P}_3(\sqrt{0.5})\mathbf{H}_3(\theta)|0_3\rangle$ (sphere) [31,32].

Ideally both the central and tomography beam splitters reflect 50% of both polarizations. In practice, we found that they deviate by a few percent and impart undesired unitary rotations on the optical modes. For the tomography beam splitter, these imperfections modified the nine measured qutrit states; we characterized this effect and incorporated it into the tomographic reconstruction. We found that the effect of the imperfect central beam splitter on the performance of the qutrit polarizer was negligible.

A frequency-doubled mode-locked Ti:Sapphire laser (820 nm $\rightarrow$ 410 nm, $\Delta\tau = 80$ fs at 82 MHz repetition rate) is used to produce photon pairs via parametric down-conversion from a Type I phase-matched 2 mm Bismuth Borate (BiBO) crystal, filtered by blocked interference filters (820 ± 1.5 nm). We collect the down-conversion into single-mode optical fibers. Photons are detected using fiber-coupled single photon counting modules and coincidences measured using a Labview (National Instruments) interfaced quad-logic card (ORTEC CO4020). When directly coupled into detectors the source yielded twofolds at 60 kHz and singles rates at 220 kHz. At the output of the complete circuit we observed fourfold coincidence rates at approximately 1 Hz.

The quality of the nonclassical interference underpinning the qutrit polarizer can be measured directly [21]. Reference [22] relates nonclassical visibilities to a Fock-state filter's ability to block single photon terms. We set all input states and measurement settings to horizontal. Twofold coincidence counts between D2 and D4 show interference between two single photons with visibility $V_{11} = 97 \pm 1\%$. Fourfolds between detectors D1–D4 detect the interference between a photon and a biphoton with visibility $V_{12} = 68 \pm 4\%$. From these visibilities we predict an extinction ratio of $5(\pm 2)$:1 [22]; i.e., our qutrit polarizer will pass the logical $|0_3\rangle$ and $|2_3\rangle$ states at 5 times the rate it passes the logical $|1_3\rangle$ state.

To demonstrate the qutrit polarizer we include a half wave plate in mode a set to $\theta = \frac{\pi}{8}$ to generate the superposition qutrit state [32]:

$$\mathbf{H}_3(\theta)|0_3\rangle = \cos^2 2\theta|0_3\rangle + \sin^2 2\theta|2_3\rangle + \sin 4\theta|1_3\rangle/\sqrt{2}. \quad (1)$$

We measure the output state in mode c without applying the qutrit polarizer. This is achieved by blocking the ancilla photon in mode b and performing qutrit tomography of mode c in twofold coincidence between D3 and D4. The experimentally reconstructed density matrix is shown in Fig. 3(a) and has a near perfect fidelity between the measured and ideal states, $F = 97 \pm 1\%$, and a low linear entropy, $S_L = 6 \pm 7\%$ [35,36]. We then prepare the output state by unblocking the ancilla and, as in all further cases, perform tomography of mode c in fourfold coincidence between D1–D4. The qutrit polarizer is now "on" and we expect the absorption of the logical $|1_3\rangle$ state. The recon-

structed density matrix is shown in Fig. 3(b) and has a lower fidelity with the ideal, $F = 78 \pm 8\%$, and linear entropy $S_L = 47 \pm 14\%$. The relative reduction in the logical $|1_3\rangle$ state probability, when the filter is turned on, yields an extinction ratio of 6.80($\pm$0.07):1, consistent with that predicted above.

Measured nonclassical visibilities are significantly limited by higher-order parametric down-conversion photon number terms [37,38]. After removing these effects, as described in Ref. [22], we find a corrected twofold visibility of $V'_{11} = 100 \pm 1\%$, which would be measured given an ideal two-photon source (higher-order effects cannot be distinguished from experimental uncertainty in the fourfold visibility). This corrected visibility can be used to predict the potential performance of our circuit given an ideal source [22]; in this case we predict that the filter would pass the logical $|0_3\rangle$ and $|2_3\rangle$ states at least 24 times the rate it passes the logical $|1_3\rangle$ state. Clearly the performance of our qutrit polarizer is significantly limited by higher-order emissions from our optical source.

Figures 3(c) and 3(d) show experimentally reconstructed density matrices of newly accessible states achieved by incorporating the qutrit polarizer with half wave plate operations applied to the initial state of $|0_3\rangle$; $|1_3\rangle$ and $(|0_3\rangle - |1_3\rangle - |2_3\rangle)/\sqrt{3}$. The fidelities with the ideal are $77 \pm 3\%$ and $83 \pm 7\%$ with linear entropies $51 \pm 7\%$ and $38 \pm 15\%$, respectively. These fidelities exceed the maximum achievable using only linear wave plates (50%) by 9 ± 1 and 5 ± 1 standard deviations, respectively.

The qutrit polarizer employs a measurement-induced nonlinearity whereby the biphoton becomes entangled with the ancilla photon. Instead of detecting the ancilla in a single, fixed polarization state, we can also use tomographic measurements to directly investigate this resultant entangled qubit-qutrit system. Without emphasis to the physical systems involved, such states were first studied by Peres as a special case of his negativity criterion for entanglement; a negativity of 0 (> 0) is conclusive of a separable (entangled) state [23,39,40]. More recently these states have received a significant amount of attention [23–28] and have been predicted to exhibit novel entanglement sudden death phenomena [29].

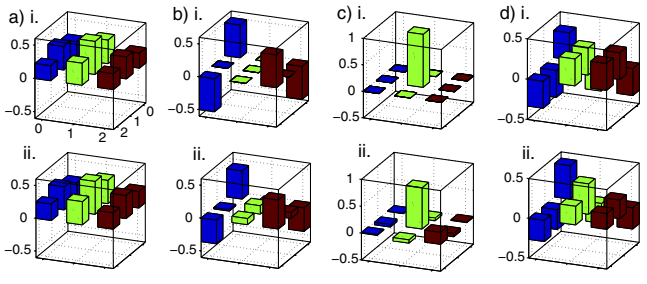

FIG. 3 (color online). Comparison of real parts of (i) ideal and (ii) measured qutrit density matrices. (a) The measured output state with the qutrit polarizer "off" [Eq. (1) for $\theta = \frac{\pi}{8}$]. (b) The output state with the qutrit polarizer "on" showing the removal of the logical $|1_3\rangle$ qutrit state. (c)–(d) Newly accessible qutrit states $|1_3\rangle$ and $(|0_3\rangle - |1_3\rangle - |2_3\rangle)/\sqrt{3}$, respectively. States (b)–(d) all lie on the surface of the sphere of Fig. 2, but not on the ring.

On injection of the qutrit state given by Eq. (1) into the Fock filter, we find the following qubit-qutrit joint state of modes c and d:

$$\frac{\cos^2 2\theta|0_2,0_3\rangle + \sin 4\theta|1_2,0_3\rangle + \sin^2 2\theta(\sqrt{2}|1_2,1_3\rangle - |0_2,2_3\rangle)}{N}, \tag{2}$$

where $N = \sqrt{2 - \cos 4\theta}$. By varying θ we can tune the level of entanglement from zero ($\theta = 0$) to near-maximal ($\theta = \frac{\pi}{4}$), with corresponding negativities of 0 to $\sqrt{8/9} \approx 0.94$, respectively. To perform qubit-qutrit state tomography we use 36 independent measurements constructed from all of the combinations of the aforementioned nine qutrit states and four qubit states (H, V, D, R). Figure 4 shows the measured density matrix for the near-maximally entangled case, which corresponds to the preparation of two vertically polarized photons in mode a. There is a high fidelity of $81 \pm 3\%$ with the ideal state and low linear entropy of $17 \pm 5\%$, and the state is highly entangled with a negativity of 0.77 ± 0.05. We note that a maximally entangled state is predicted for $\theta = \frac{\pi}{4}$ and a central beam splitter reflectivity of $R = \sqrt{2}/(\sqrt{2} + 1) \approx 58.6\%$.

Entangling information carriers to ancilla qubits is an extremely powerful technique [41]: such correlations play a central role in the power of the Fock filter to transform biphotonic qutrits. However, the application of our technique is not limited to extending transforms on single qutrits. We propose that the generation of qubit-qutrit entanglement offers a path to realize multiqutrit operations. For example, a pair of entangled qubit-qutrit states could be used to create qutrit-qutrit entanglement by projecting the qubits into an entangled state using well-known techniques. The much anticipated development of high-brightness single photon sources will make such experiments feasible in the near future. We wish to emphasize that our technique is not limited to manipulating biphotons. The Fock filter can be applied to any system where measurement can induce nonlinear effects, that is, any bosonic encoding of quantum information, including bosonic atoms [42] and time-bin, frequency, and orbital angular momentum encoding of photons.

We have shown that measurement-induced nonlinearities offer significant advantages for the manipulation of higher dimensional bosonic information carriers, specifically biphotonic qutrits. We demonstrated a nonlinear qutrit polarizer, capable of conditionally removing a single logical qutrit state from a superposition and greatly extending the range of possible qutrit transforms. Such tools could find application to quickly generate the mutually unbiased basis states required for optimum security in qutrit quantum-key-distribution protocols [5–7] or as a filtering technique to manipulate entanglement in qutrit-

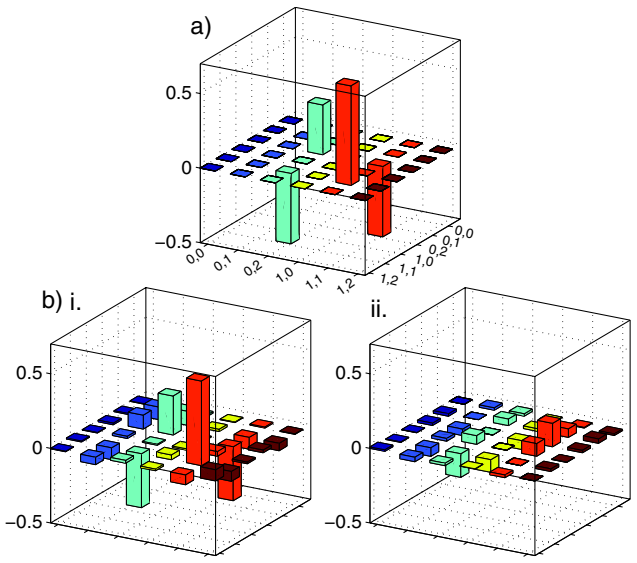

FIG. 4 (color online). Comparison of entangled qubit-qutrit density matrices. (a) Ideal, (b) and (c) measured real and imaginary parts. There is a high fidelity of (81 ± 3%) with the ideal state and low linear entropy (17 ± 5%), and the state is highly entangled with a negativity of 0.77 ± 0.05. The ideal state is given by Eq. (2) for $\theta = \pi/4$. Note the axis label: x,j represents the qubit logical state x and the qutrit logical state j, i.e., $|x_2, j_3\rangle$.

qutrit states. Finally we fully characterized the entangled photon-biphoton state that underpins the power of our technique. This is the first instance of the generation and characterization of entanglement between these distinct physical systems and makes recent theoretical proposals experimentally testable [29]. Besides offering a path to implement novel multiqutrit operations we propose that our technique can be extended to manipulate any bosonic encoding of quantum information.

This work was supported by the Australian Research Council, ARC Discovery Federation, DEST Endeavour Europe programs, and the IARPA-funded U.S. Army Research Office Contract No. W911NF-05-0397.

Note added.—Recently several proposals were presented to which our technique is directly relevant [43–45].

[1] N. K. Langford *et al.*, Phys. Rev. Lett. **93**, 053601 (2004).
[2] R. W. Spekkens and T. Rudolph, Phys. Rev. A **65**, 012310 (2001).
[3] G. Molina-Terriza *et al.*, Phys. Rev. Lett. **92**, 167903 (2004).
[4] S. Gröblacher *et al.*, New J. Phys. **8**, 75 (2006).
[5] D. Bruß and C. Macchiavello, Phys. Rev. Lett. **88**, 127901 (2002).
[6] N. J. Cerf *et al.*, Phys. Rev. Lett. **88**, 127902 (2002).
[7] T. Durt *et al.*, Phys. Rev. A **67**, 012311 (2003).
[8] M. Fujiwara *et al.*, Phys. Rev. Lett. **90**, 167906 (2003).
[9] D. Collins *et al.*, Phys. Rev. Lett. **88**, 040404 (2002).
[10] D. Kaszlikowski *et al.*, Phys. Rev. A **65**, 032118 (2002).
[11] T. C. Ralph, K. Resch, A. Gilchrist, Phys. Rev. A **75**, 022313 (2007).
[12] Y. I. Bogdanov *et al.*, Phys. Rev. Lett. **93**, 230503 (2004).
[13] A. Mair *et al.*, Nature (London) **412**, 313 (2001).
[14] Y. Bogdanov *et al.*, arXiv:quant-ph/0411192v1.
[15] Y. I. Bogdanov *et al.*, Phys. Rev. A **70**, 042303 (2004).
[16] G. Vallone *et al.*, Phys. Rev. A **76**, 012319 (2007).
[17] A. Grudka and A. Wojcik, Phys. Rev. A **66**, 064303 (2002).
[18] H. F. Hofmann and S. Takeuchi, Phys. Rev. Lett. **88**, 147901 (2002).
[19] X. Zou, K. Pahlke, and W. Mathis, Phys. Rev. A **66**, 064302 (2002).
[20] K. Sanaka *et al.*, Phys. Rev. Lett. **92**, 017902 (2004).
[21] K. Sanaka, K. J. Resch, and A. Zeilinger, Phys. Rev. Lett. **96**, 083601 (2006).
[22] K. J. Resch *et al.*, Phys. Rev. Lett. **98**, 203602 (2007).
[23] A. Peres, Phys. Rev. Lett. **77**, 1413 (1996).
[24] P. B. Slater, Phys. Rev. A **71**, 052319 (2005).
[25] A. Cabello, A. Feito, and A. Lamas-Linares, Phys. Rev. A **72**, 052112 (2005).
[26] O. Osenda and G. A. Raggio, Phys. Rev. A **72**, 064102 (2005).
[27] S. Jami andM. Sarbishei, arXiv:quant-ph/0606039.
[28] P. B. Slater, arXiv:quant-ph/0702134.
[29] K. Ann and G. Jaeger, arXiv:quant-ph/0707.4485.
[30] C. K. Hong, Z. Y. Ou, and L. Mandel, Phys. Rev. Lett. **59**, 2044 (1987).
[31] For our Fock filter with reflectivity $R = r^2$,

$$\mathbf{P}_3(r) = \begin{bmatrix} r(2-3r^2 & 0 & 0 \\ 0 & r(1-2r^2) & 0 \\ 0 & 0 & -r^3 \end{bmatrix}.$$

[32] From Ref. [15], the wave plate action on a qutrit is

$$\begin{bmatrix} t^2 & \sqrt{2}tr & r^2 \\ -\sqrt{2}tr^* & |t|^2 - |r|^2 & \sqrt{2}t^* r \\ r^{*2} & -\sqrt{2}t^* r^* & t^{*2} \end{bmatrix},$$

where $t = \cos\delta + i\sin\delta\cos 2\theta$, $r = i\sin\delta\sin 2\theta$, and θ is the wave plate angle. For a half wave plate, $\mathbf{H}_3(\theta)$, $\delta = \pi/2$; for a quarter-wave plate, $\mathbf{Q}_3(\theta)$, $\delta = \pi/4$.
[33] A. Doherty and A. Gilchrist (to be published).
[34] J. L. O'Brien *et al.*, Phys. Rev. Lett. **93**, 080502 (2004).
[35] Fidelity is $F(\rho, \sigma) \equiv \{\mathrm{Tr}[\sqrt{\sqrt{\rho}\sigma\sqrt{\rho}}]\}^2$; linear entropy is $S_L \equiv d(1 - \mathrm{Tr}[\rho^2])/(d-1)$, where d is the state dimension.
[36] A. G. White *et al.*, J. Opt. Soc. Am. B **24**, 172 (2007).
[37] J. Fulconis *et al.*, Phys. Rev. Lett. **99**, 120501 (2007).
[38] T. J. Weinhold *et al.*, (to be published).
[39] T. Wei *et al.*, Phys. Rev. A **67**, 022110 (2003).
[40] We define negativity, following [39], as $N = \max\{0, -2 * \sum_i \lambda_i\}$, where λ_i are the negative eigenvalues of the partial transpose of the target density matrix.
[41] E. Knill *et al.*, Nature (London) **409**, 46 (2001).
[42] S. Popescu, Phys. Rev. Lett. **99**, 130503 (2007).
[43] I. Bregman *et al.*, arXiv:quant-ph/0709.3804.
[44] C. Bishop and M. S. Byrd, arXiv:quant-ph/0709.0021.
[45] M. Ali *et al.*, arXiv:0710.2238.